

Gravitational collapse in general relativity and its extensions

Author: Gerard Carol Raventós, gerardcarol20@gmail.com
Facultat de Física, Universitat de Barcelona, Diagonal 645, 08028 Barcelona, Spain.

Advisor: Pablo Antonio Cano Molina Niñirola, pablo.cano@ub.edu

Abstract: General Relativity predicts the formation of singularities in black holes. These singularities signal a breakdown of the theory and suggest the need for a new approach that resolves this issue. In this work, we explore modifications of General Relativity through infinite higher-order curvature corrections, leading to regular black holes. We review the dynamics of gravitational collapse using the thin-shell formalism in D -dimensional spacetimes, focusing on both the Schwarzschild and regular Hayward black holes. Two matter models are considered: pressureless dust and matter subject to a pressure $p = \omega\sigma$. Through analytical and numerical analysis, we characterize the effective potential governing the shell evolution and identify conditions under which gravitational collapse is halted. We show that, in contrast to the singular Schwarzschild case, the collapse of the shell does not give rise to a singularity when using the Hayward metric and even presents an inaccessible region near $R = 0$ under pressure. These results contribute to the understanding of regular black hole formation dynamics and highlight the relevance of higher-order gravitational corrections in resolving singularities.

Keywords: General relativity, black holes, singularities, modified gravity.

SDGs: Quality Education (SDG 4), Industry, Innovation and Infrastructure (SDG 9).

I. INTRODUCTION

Einstein's theory of General Relativity is the starting point of all modern understanding of gravity. However, it has open problems, as it predicts the existence of singularities (points where physical quantities such as curvature become infinite). In fact, singularities are intrinsically linked to Einstein's theory of General Relativity, as demonstrated by Penrose-Hawking Singularity Theorems [1, 2].

From a theoretical viewpoint, General Relativity is an incomplete theory, as it does not account for quantum effects. The easiest solution for a black hole in this theory is the Schwarzschild solution [3], which describes a region of spacetime from which nothing inside can escape, with a singularity towards where everything collapses. Any observer inside a black hole will reach the singularity in a finite amount of proper time, and beyond this point the theory experiments a breakdown, as nothing else can be described after it has been reached. It is widely expected that these singularities will not occur in nature and will be resolved by a more complete framework, likely involving quantum gravitational effects.

The first attempts to find theories that describe regular black holes (i.e., black holes without singularities) date back to 1968 [4] and were further refined using non-linear theories of electrodynamics [5]. These attempts, however, have some inconsistencies, as they require charge and exotic matter [6, 7].

Other approaches to try to resolve singularities are the addition of higher-order derivative correction terms to the Einstein-Hilbert action. These type of theories try to resolve singularities using a pure gravitational approach. In this line of work, perhaps some of the most interesting theories are quasi-topological theories of gravity, which

are theories for dimensions $D \geq 5$ that introduce higher-order curvature correction terms with the property that they greatly simplify solutions but maintain a high degree of generality [8, 9].

In [10] it was shown that, by introducing an infinite tower of correction terms in the Einstein-Hilbert action, the singularity can be resolved. Even more, it was shown that the solutions that were found are the only static and spherically symmetric solutions of the corresponding theory.

Furthermore, in [11] the dynamics of the formation of regular black holes in these theories was studied using a thin-shell approach for pressureless matter. One of the most relevant aspects of this study is that it was not only done in general, but it also provided several concrete examples. The easiest (and probably the most known) of these examples is the Hayward D -dimensional black hole (for odd D).

In this work we review the dynamics of the formation of Schwarzschild and Hayward black holes from the collapse of a thin shell when there is a pressure of the type $p = \omega\sigma$, where σ is the surface matter density and ω is a constant parameter.

II. HIGHER-ORDER CORRECTIONS

In the usual theory of general relativity for a D -dimensional spacetime, Einstein's field equations are derived from the Einstein-Hilbert action

$$S = \frac{1}{16\pi G_N} \int d^D x \sqrt{|g|} R. \quad (1)$$

The static and spherically symmetric (in vacuum conditions) solution corresponding to this theory is the

Schwarzschild solution, described by

$$ds^2 = -f(r)dt^2 + \frac{dr^2}{f(r)} + r^2 d\Omega_{D-2}^2, \quad (2)$$

where $f(r) = 1 - 2M/r^{D-3}$.

This solution presents an event horizon at $r_S = (2M)^{\frac{1}{D-3}}$ and a singularity at $r = 0$.

In [10] they tried to find a modified theory of gravity by supplementing the Einstein-Hilbert action with an infinite sum of higher-order correction terms:

$$S = \frac{1}{16\pi G_N} \int d^D x \sqrt{|g|} \left[R + \sum_{n=2}^{\infty} \alpha_n \mathcal{Z}_n \right]. \quad (3)$$

α_n are coupling constants with dimensions of $\text{length}^{2(n-1)}$, and the correction terms \mathcal{Z}_n can be found explicitly in [10, 11]. It was shown that these new theories resolve black hole singularities.

Not only this, but it was also shown that spherically symmetric static solutions of these theories are described by

$$ds^2 = -f(r)dt^2 + \frac{dr^2}{f(r)} + r^2 d\Omega_{D-2}^2 \quad (4)$$

and must satisfy

$$h(\psi) = \frac{2M}{r^{D-1}}, \quad (5)$$

where

$$h(\psi) = \psi + \sum_{n=2}^{\infty} \alpha_n \frac{D-2n}{D-2} \psi^n, \quad \psi = \frac{1-f(r)}{r^2} \quad (6)$$

and if M is the ADM mass,

$$M := \frac{8\pi G_N M}{(D-2)\Omega_{D-2}}. \quad (7)$$

Some sufficient conditions for the coupling constants so the singularity is resolved can be found in subsection A of the supplementary material.

Under these assumptions, the Schwarzschild solution is recovered choosing $\alpha_n = 0 \forall n$ (i.e., not adding any correction term to the Einstein-Hilbert action), as (6) and (5) yield $h(\psi) = \psi$ and $f(r) = 1 - 2M/r^{D-3}$.

The D -dimensional Hayward black hole solution is the easiest solution that rises from a theory of this type that describes a non-singular black hole. It arises from taking $\alpha_n = [(D-2)/(D-2n)]\alpha^n$, where $\alpha > 0$ is a constant parameter. Now, (6) and (5) become

$$h(\psi) = \frac{\psi}{1 - \alpha\psi} \quad (8)$$

and

$$f(r) = 1 - \frac{2Mr^2}{r^{D-1} + 2M\alpha}. \quad (9)$$

The horizon structure for the Hayward black hole is slightly more difficult than the Schwarzschild's one. This regular black hole can have 0, 1 or 2 horizons depending on the value of M (which determines the number of zeroes of (9)). More precisely, it depends on

$$M_{critical} = \frac{D-1}{4} \left(\frac{D-1}{D-3} \alpha \right)^{\frac{D-3}{2}}. \quad (10)$$

For $M > M_{critical}$ there will be two horizons, for $M = M_{critical}$ there will be one extremal horizon, and for $M < M_{critical}$ there will be no horizons at all.

III. THIN SHELL FORMALISM

In this section we will follow the work of [11] when studying the collapse of a thin shell of matter (which can be viewed as a hypersurface Σ) in these modified theories of gravity. The interior of the shell ($-$) is Minkowskian, and thus, described by

$$ds_-^2 = -dt_-^2 + dr^2 + r^2 d\Omega_{D-2}^2. \quad (11)$$

The exterior ($+$), however, is described by

$$ds_+^2 = -f(r)dt_+^2 + \frac{dr^2}{f(r)} + r^2 d\Omega_{D-2}^2. \quad (12)$$

To join the two solutions, the generalized Israel junction conditions must be used, which can be written as

$$h_{AB}^+ = h_{AB}^-, \quad (13)$$

where h_{AB}^+ and h_{AB}^- are the induced metric at each side of the shell (and the capital indices indicate that we are referring to the boundary indices), and

$$\Pi_{AB}^- - \Pi_{AB}^+ = 8\pi G_N S_{AB}. \quad (14)$$

S_{AB} is the surface stress-energy tensor and Π_{AB} (which represents the boundary equations of motion) satisfies

$$\Pi_{\tau\tau} = \frac{D-2}{r} \int_0^\beta dz h' \left(\frac{1 + \dot{r}^2 - z^2}{r^2} \right) \quad (15)$$

and

$$g^{ij}\Pi_{ij} = -\frac{1}{r^{D-3}\dot{r}} \frac{d}{d\tau} (r^{D-2}\Pi_{\tau\tau}), \quad (16)$$

where n is the normal vector of Σ , $\beta := n^\mu \partial_\mu r$ and $\dot{r} = dr/d\tau$.

By parametrizing the shell in terms of the proper time $t_\pm = T_\pm(\tau)$ and $r = R(\tau)$ and imposing the continuity of the metric at Σ , $ds_{\Sigma-}^2 = ds_{\Sigma+}^2 = -d\tau^2 + R^2 d\Omega_{D-2}^2$, one can see that $\beta_- = \dot{T}_- = \sqrt{1 + \dot{R}^2}$ and $\beta_+ = f(R)\dot{T}_+ =$

$\pm\sqrt{f(R) + \dot{R}^2}$ (the sign of β_+ is positive outside the black hole, and then it must be changed every time $\beta_+ = 0$). Then, equation (16) can be rewritten as

$$\Pi_{\tau\tau}^- - \Pi_{\tau\tau}^+ = 8\pi G_N S_{\tau\tau} \quad (17)$$

and

$$-\frac{1}{R^{D-3}\dot{R}}\frac{d}{d\tau}[R^{D-2}(\Pi_{\tau\tau}^- - \Pi_{\tau\tau}^+)] = 8\pi G_N g^{ij} S_{ij}. \quad (18)$$

By considering the shell as a perfect fluid, the stress-energy tensor can be written as

$$S_{AB} = (\sigma + p)u_A u_B + p h_{AB}, \quad (19)$$

where u_A is the field of velocities of the shell. The induced metric on the shell is described by $h_{\tau\tau} = -1$ and $h_{ij} = R^2 \gamma_{ij}$, as τ is the proper time of the shell (where γ_{ij} is the metric of the $(D-2)$ -dimensional sphere).

Equation (17) is

$$\Pi_{\tau\tau}^- - \Pi_{\tau\tau}^+ = 8\pi G_N \sigma, \quad (20)$$

and equation (18) can be written as

$$(D-2)p = \frac{-1}{R^{D-3}\dot{R}}\frac{d}{d\tau}[R^{D-2}\sigma]. \quad (21)$$

Just by using these two equations, we will be able to find an effective potential for the shell, i.e. will find an equation of the type

$$\dot{R}^2 + V(R) = 0. \quad (22)$$

A. Pressureless matter

In the case of pressureless matter, equation (21) with $p = 0$ yields that $R^{D-2}\sigma$ is a constant, so one can define the constant $m := \sigma R^2 \Omega_{D-2}$ and, by defining

$$m = \frac{8\pi G_N m}{(D-2)\Omega_{D-2}} \quad (23)$$

and using equations (15) and (20), one gets

$$\frac{m}{R^{D-3}} = \int_{\beta_+}^{\beta_-} dz h' \left(\frac{1 + \dot{R}^2 - z^2}{R^2} \right). \quad (24)$$

From this equation, we will be able to derive the effective potential of the shell in the pressureless case.

B. Pressure $p = \omega\sigma$

In the case that matter is subject to a pressure of the type $p = \omega\sigma$, equation (21) is

$$(D-2)\omega\sigma = \frac{-1}{R^{D-3}\dot{R}}\frac{d}{d\tau}[R^{D-2}\sigma], \quad (25)$$

which yields

$$\sigma = \frac{\kappa}{R^{(D-2)(\omega+1)}}, \quad (26)$$

where κ is a constant. Substituting this in equation (20) and using equation (15) one finds

$$\int_{\beta_+}^{\beta_-} dz h' \left(\frac{1 + \dot{R}^2 - z^2}{R^2} \right) = \frac{8\pi G_N \kappa}{(D-2)R^{(D-2)(\omega+1)-1}}. \quad (27)$$

As in the previous subsection, this equation will enable us to describe the dynamics of the shell.

IV. RESULTS

A. Dynamics of the Schwarzschild solution

For Einstein gravity, the exterior spacetime is given by the Schwarzschild metric, while the interior of the shell will be Minkowskian. As such, if the matter of the shell is pressureless, as $h'(\psi) = 1$, equation (24) yields

$$V(R) = -\frac{M}{R^{D-3}} - \frac{m^2}{4R^{2(D-3)}} - \frac{M^2}{m^2} + 1. \quad (28)$$

In this case the potential always decreases with decreasing values of R , tends to $-\infty$ when $R \rightarrow 0$ and is asymptotic to $1 - (M/m)^2$ as $R \rightarrow \infty$ (Figure 4 in Supplementary Material). If the shell starts at rest at any value of R , it will end up as a Schwarzschild black hole.

However, if one considers that this matter is subject to a pressure of the type $p = \omega\sigma$, then equation (27) yields a potential of the type

$$V(R) = -\frac{M}{R^{D-3}} - \frac{\tilde{\kappa}^2}{4R^{2(D-2)(\omega+1)-2}} - \frac{M^2 R^{2\omega(D-2)}}{\tilde{\kappa}^2} + 1, \quad (29)$$

where

$$\tilde{\kappa} = \frac{8\pi G_N \kappa}{D-2}. \quad (30)$$

Under these circumstances, the effective potential always has a maximum and diverges to $-\infty$ at $R \rightarrow 0$ and at $R \rightarrow \infty$ (see Figure 1). If this maximum is greater than the total energy of the shell (which, by definition of V , is always 0), and the shell starts at any valid value of R (i.e., where $V(R) \leq 0$) with R greater than the radius corresponding to the maximum of V , the collapse will not occur (thanks to the pressure) and the shell will bounce off and proceed to expand infinitely. However, if it starts at any valid value of R with R smaller than the radius corresponding to the maximum of V , the collapse will not be stopped. If the maximum of the potential is below 0 and $R < 0$, the collapse will also occur, and thus the formation of the Schwarzschild black hole will

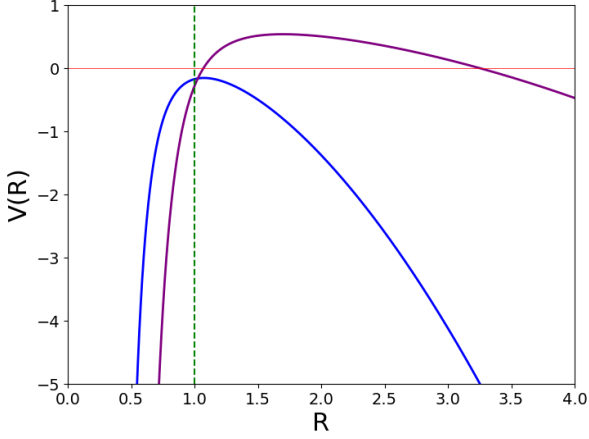


FIG. 1: Effective potential $V(R)$ depending on the radius of the shell R when it is subjected to a pressure of the type $p = \omega\sigma$ for the Schwarzschild case (29). The values used are $D = 5$, $\omega = 1/3$, $M = 0.5$ for the two plots, and $\tilde{\kappa} = 5$ for the purple plot and $\tilde{\kappa} = 2$ for the blue plot. The vertical green line is the Schwarzschild radius and the horizontal red line at $V(R) = 0$ is the total energy of the shell (which is fixed to 0 by definition of V).

happen independently of the starting radius of the shell. Instead, if again the maximum of the potential is below 0 and now $R > 0$, the shell will expand infinitely (the relationship between M and $\tilde{\kappa}$ so that the maximum is exactly at $V_{max} = 0$ can be seen in Figure 5).

B. Dynamics of the Hayward solution

If one considers the modified theory of gravity that gives rise to the Hayward black hole solution, the interior of the shell will still be Minkowskian, but the exterior will be described by the Hayward solution. Now, for the pressureless case, equation (24) when integrated becomes

$$m = \frac{R^{D-1}}{2(R^2 - \alpha\beta_-^2)} \left(\beta_- - \left(1 + \frac{2\alpha M}{R^{D-1}} \right) \beta_+ + \frac{R^2 \arctan \left(\frac{(\beta_- - \beta_+) \sqrt{\alpha(R^2 - \alpha\beta_-^2)}}{R^2 - \alpha\beta_- (\beta_- - \beta_+)} \right)}{\sqrt{\alpha(R^2 - \alpha\beta_-^2)}} \right). \quad (31)$$

This equation cannot be solved algebraically to find an equation of the type (22). Instead, one can approximate it using numerical methods, which yields an effective potential as in Figure 2.

The potential tends to a constant when $R \rightarrow \infty$ and when $R \rightarrow 0$, and it has an absolute minimum. If $M < m$ (e.g., the shell starts at rest at any value of $R \neq 0, \infty$), the shell will not be able to reach $R = 0$ and will bounce after passing the potential minimum. If $M = m$ (e.g., the shell starts at rest at infinity), as in Figure 2, the

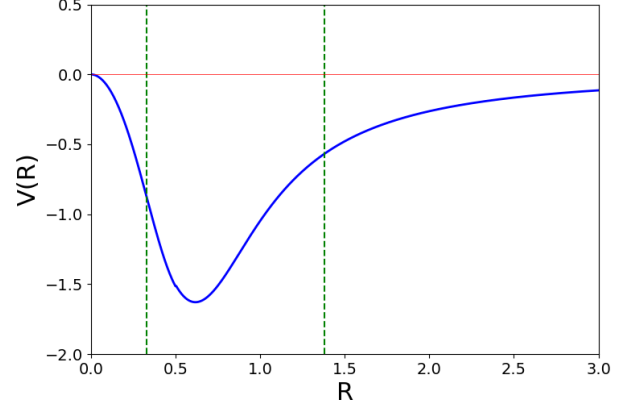


FIG. 2: Effective potential $V(R)$ depending on the radius of the shell R for the pressureless Hayward case (31). The values used are $D = 5$, $\alpha = 0.1$, $M = 1$ and $m = 1$. The vertical green lines are the two horizon radii and the horizontal red line at $V(R) = 0$ is the total energy of the shell.

shell will be able to approach $R = 0$, and will reach it in an infinite amount of time. Finally, if $M > m$ (e.g., if it starts at infinity with some kinetic energy), it will be able to reach $R = 0$ in a finite amount of time (the particles, as under this assumptions do not interact, will not have any trouble reaching $R = 0$, and their motion can be continued using antipodal identification).

If one considers matter under a pressure of the type $p = \omega\sigma$, equation (27) becomes

$$\frac{8\pi G_N \kappa}{D-2} = \frac{R^{(D-2)(\omega+1)+1}}{2(R^2 - \alpha\beta_-^2)} \left(\beta_- - \left(1 + \frac{2\alpha M}{R^{D-1}} \right) \beta_+ + \frac{R^2 \arctan \left(\frac{(\beta_- - \beta_+) \sqrt{\alpha(R^2 - \alpha\beta_-^2)}}{R^2 - \alpha\beta_- (\beta_- - \beta_+)} \right)}{\sqrt{\alpha(R^2 - \alpha\beta_-^2)}} \right). \quad (32)$$

As before, this cannot be solved algebraically, and numerical methods for the approximation of its solutions must be used.

Under these assumptions, the effective potential always diverges when $R \rightarrow \infty$, and it always tends to 1 when $R \rightarrow 0$ (Figure 3). Depending on the relationship between the different values of the constants (Figure 7 in Supplementary Material), the effective potential can present a minimum and a maximum. For a given value of α , if M is sufficiently smaller than κ , then the effective potential will present the maximum (and minimum), which will be above 0 (Figure 6 in Supplementary Material), so there is an inaccessible region for the shell (which always appears before the first horizon), and thus if the shell starts at a value of R larger than the maximum radius of the inaccessible region, it will not collapse and form a black hole, as it will bounce off and then expand infinitely. In this case, the collapse is stopped by the pressure of the shell. However, if M is large enough

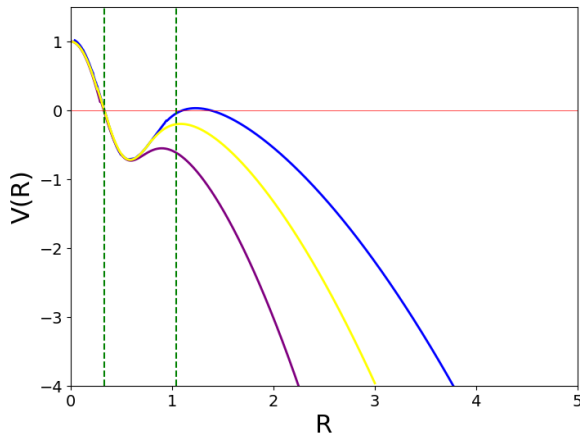


FIG. 3: Effective potential $V(R)$ for three different values of the constant κ depending on the radius of the shell R when it is subjected to a pressure of the type $p = \omega\sigma$ for the Hayward case (32). The values used are $D = 5$, $\omega = 1/3$, $\alpha = 0.1$ and $M = 0.59$ for the three plots and $\kappa = 0.6$ for the purple plot, $\kappa = 0.8$ for the yellow plot and $\kappa = 1$ for the blue plot. The vertical green lines are the two horizon radii and the horizontal red line at $V(R) = 0$ is the total energy of the shell.

(compared to κ), then this maximum will be below 0 or might not appear at all (and thus the minimum neither), meaning that the shell will be able to pass the first horizon and the black hole will form. After creating this black hole, the shell will continue to shrink until it reaches $V = 0$ and bounces off, expanding indefinitely and thus passing again the first horizon, vanishing the black hole and emerging into a "new Universe" (a similar process happens in the pressureless Hayward black hole, as seen in [11]). In this case, in contrast to the last explained bounce, this one is caused by the higher-order correction terms of the curvature.

Regarding the limit $R \rightarrow 0$, the fact that the potential always tends to 1 shows that the total collapse will never be reached ($V \rightarrow 1$ when $R \rightarrow 0$ independently of the values of the constants, the only change is that the inaccessible region is narrower or wider). In addition, the bounce will always happen after the shell has crossed the inner horizon.

V. CONCLUSIONS

It has been shown that (as already known), the collapse in the Schwarzschild case cannot be stopped by the matter's pressure if M is large enough, and the formation of a singular black hole will occur. However, in the theory that yields the Hayward solution by introducing higher-order correction terms, it has been shown that even if the pressure is not enough to stop the formation of the black hole, it will not create a singularity. In fact, we have seen that $R = 0$ is never reached for a thin shell with non-zero pressure. As seen in Figure 3, the smoothness of the potential is still recovered at $R = 0$, even if this point can never be reached by the shell.

As future work, a more extensive analysis could be done, further exploring the relationship between the constants and their impact on the dynamics of the shell, while also using more potent machinery, as the computational cost for finding these solutions has been quite high for our machines.

Acknowledgments

I would like to thank my advisor, Pablo Antonio Cano Molina Niñirola, for his valuable mentoring during this project. I would also like to thank my family and friends, who have supported me during this project.

-
- [1] R. Penrose, Gravitational collapse and space-time singularities, *Phys. Rev. Lett.* **14**, (1965) 57–59.
 - [2] S. W. Hawking and G. F. R. Ellis, *The Large Scale Structure of Space-Time*, Cambridge Monographs on Mathematical Physics, Cambridge University Press, 2nd ed. (2023).
 - [3] K. Schwarzschild, Über das Gravitationsfeld eines Massenpunktes nach der Einsteinschen Theorie, *Sitzungsberichte der Königlich Preussischen Akademie der Wissenschaften*, 1916, **7**, 189–196.
 - [4] J. Bardeen, Non-singular general relativistic gravitational collapse, in *Proceedings of the 5th International Conference on Gravitation and the Theory of Relativity*, (Sep. 1968) p. 87.
 - [5] E. Ayón-Beato and A. García, Regular Black Hole in General Relativity Coupled to Nonlinear Electrodynamics, *Phys. Rev. Lett.* **80** (1998) 5056–5059.
 - [6] V. P. Frolov, Notes on non-singular models of black holes, *Phys. Rev. D* **94** (2016) 104056.
 - [7] C. Lan, H. Yang, Y. Guo, and Y.-G. Miao, Regular Black Holes: A Short Topic Review, *Int. J. Theor. Phys.* **62** (2023) 46.
 - [8] J. Oliva and S. Ray, A new cubic theory of gravity in five dimensions: black hole, Birkhoff's theorem and C-function, *Class. Quantum Grav.* **27** (2010) 225002.
 - [9] R. C. Myers and B. Robinson, Black holes in quasi-topological gravity, *J. High Energy Phys.* **08** (2010) 067.
 - [10] P. Bueno, P. A. Cano, and R. A. Hennigar, Regular black holes from pure gravity, *Phys. Lett. B* **861** (2025) 139260.
 - [11] P. Bueno, P. A. Cano, R. A. Hennigar, and Á. J. Murcia, Regular black holes from thin-shell collapse, *Phys. Rev. D* **111** (2025) 104009.

Col·lapse gravitacional en relativitat general i les seves extensions

Author: Gerard Carol Raventós, gerardcarol20@gmail.com
 Facultat de Física, Universitat de Barcelona, Diagonal 645, 08028 Barcelona, Spain.

Advisor: Pablo Antonio Cano Molina Niñirola, pablo.cano@ub.edu

Resum: La relativitat general prediu la formació de singularitats en els forats negres. Aquestes singularitats indiquen un error de la teoria i suggereixen la necessitat d'un nou enfocament que resolgui aquest problema. En aquest treball, explorem modificacions de la relativitat general mitjançant correccions infinites d'ordre superior en la curvatura, que condueixen a forats negres regulars. Revisem la dinàmica del col·lapse gravitacional utilitzant el formalisme de la closca prima (*thin-shell* en anglès) en espais D -dimensionals, centrant-nos tant en els forats negres clàssics de Schwarzschild com en els forats negres regulars de Hayward. Es consideren dos models de matèria: pols sense pressió i matèria sotmesa a una pressió $p = \omega\sigma$. Mitjançant anàlisis analítica i numèrica, caracteritzem el potencial efectiu que governa l'evolució de la closca i identifiquem les condicions sota les quals el col·lapse gravitacional s'atura. Mostrem que, en contrast amb el cas singular de Schwarzschild, la solució de Hayward preserva la seva no-singularitat i fins i tot presenta una regió inaccessible propera a $R = 0$ sota pressió. Aquests resultats contribueixen a la comprensió de la dinàmica de formació dels forats negres regulars i ressalten la rellevància de les correccions gravitacionals d'ordre superior en la resolució de singularitats.

Paraules clau: Relativitat general, forats negres, singularitats, gravetat modificada.

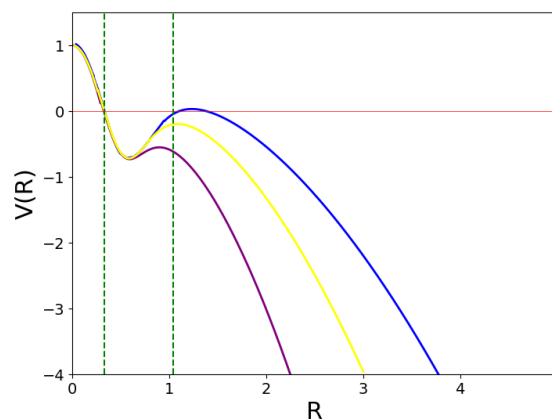
ODSs: Aquest TFG està relacionat amb els Objectius de Desenvolupament Sostenible (SDGs) 4-Educació de qualitat, i 9-Indústria, innovació, infraestructures.

Objectius de Desenvolupament Sostenible (ODSs o SDGs)

1. Fi de les desigualtats		10. Reducció de les desigualtats	
2. Fam zero		11. Ciutats i comunitats sostenibles	
3. Salut i benestar		12. Consum i producció responsables	
4. Educació de qualitat	X	13. Acció climàtica	
5. Igualtat de gènere		14. Vida submarina	
6. Aigua neta i sanejament		15. Vida terrestre	
7. Energia neta i sostenible		16. Pau, justícia i institucions sòlides	
8. Treball digne i creixement econòmic		17. Aliança pels objectius	
9. Indústria, innovació, infraestructures	X		

El contingut d'aquest TFG del grau universitari en Física, està relacionat amb l'ODS 4, ja que contribueix a l'educació a nivell universitari i a l'interpretació de la dinàmica del col·lapse de forats negres regulars, i amb l'ODS 9, ja que ajuda a la innovació en el camp, estudiant el col·lapse de forats negres regulars en el cas que la matèria es troba sotmesa a una pressió.

GRAPHICAL ABSTRACT



SUPPLEMENTARY MATERIAL

A. Sufficient conditions for the coupling constants

Some sufficient conditions for the singularity to be resolved are

$$\alpha_n(D - 2n) \geq 0 \quad \forall n, \quad \lim_{n \rightarrow \infty} |\alpha_n|^{\frac{1}{n}} = C > 0, \quad (33)$$

as when $r \rightarrow 0$, f can be approximated as

$$f(r) \sim 1 - \left(\frac{2M}{\alpha_{\tilde{n}}} \right)^{1/\tilde{n}} r^{2-(D-1)/\tilde{n}} + \dots \quad (34)$$

for $\tilde{n} \rightarrow \infty$. Since $\psi_0 := 1/C$ is the convergence radius of the series found in (6) (for $\psi > 0$), $h(\psi_0)$ must diverge, and thus by equation (5), when $r \rightarrow 0$ then $\psi \rightarrow \psi_0$, which means that using (34) we can describe f as $f \sim 1 - \psi_0 r^2 + \dots$. This means that f is (at least) \mathcal{C}^2 , which implies that the Riemmanian curvature will be finite.

B. Plots

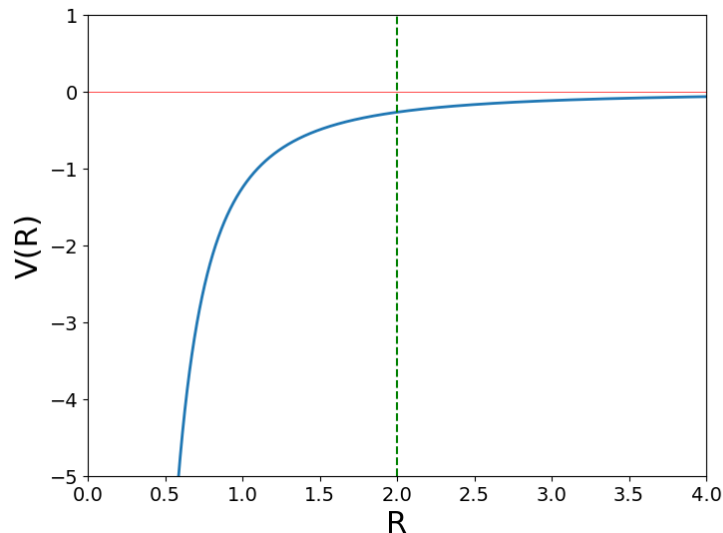


FIG. 4: Effective potential $V(R)$ depending on the radius of the shell R using the pressureless equation for the Schwarzschild case (28). The values used are $D = 5$, $M = 1$ and $\mathfrak{m} = 1$. The vertical green line is the Schwarzschild radius and the horizontal red line at $V(R) = 0$ is the total energy of the shell.

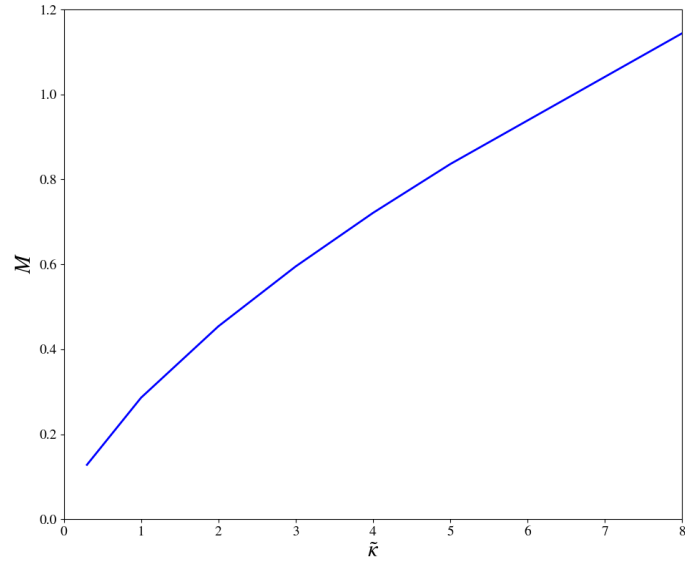


FIG. 5: Relationship between M and $\tilde{\kappa}$ in the Schwarzschild case with pressure $p = \omega\sigma$ when the maximum of the potential is $V_{max} = 0$ (i.e., the limit where the collapse is still halted by pressure), using equation (29) for $D = 5$, $\alpha = 0.1$ and $\omega = 1/3$.

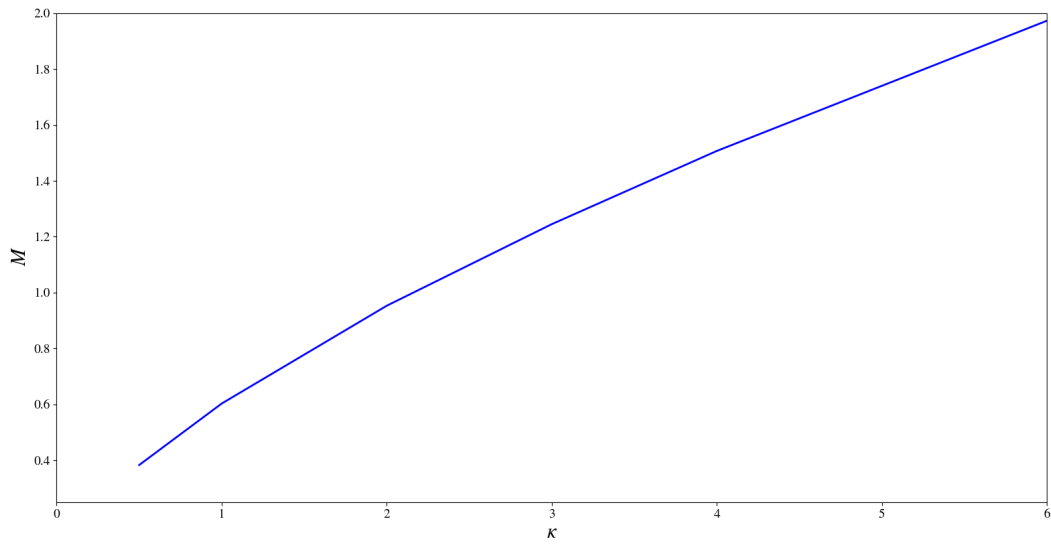


FIG. 6: Relationship between M and κ in the Hayward case with pressure $p = \omega\sigma$ when the maximum of the potential is $V_{max} = 0$ (i.e., the limit where the collapse is halted and the shell doesn't pass the first horizon), using equation (32) for $D = 5$, $\alpha = 0.1$ and $\omega = 1/3$.

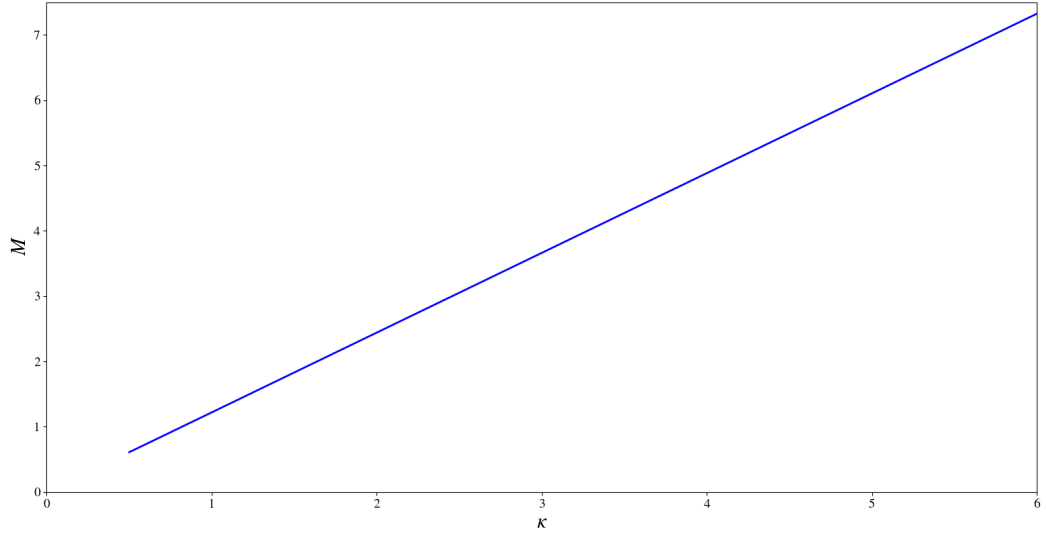


FIG. 7: Relationship between M and κ in the Hayward case with pressure $p = \omega\sigma$ in the limit where the potential starts to present a maximum (and thus, also a minimum) using equation (32) for $D = 5$, $\alpha = 0.1$ and $\omega = 1/3$.